THE ASTROPHYSICAL JOURNAL, 369:L45–L49, 1991 March 10

THE POSTCOLLAPSE CORE OF M15 IMAGED WITH THE *HST* PLANETARY CAMERA[1]

TOD R. LAUER,[2] JON A. HOLTZMAN,[3] S. M. FABER,[4] WILLIAM A. BAUM,[5] DOUGLAS G. CURRIE,[6] S. P. EWALD,[7]
EDWARD J. GROTH,[8] J. JEFF HESTER,[9] T. KELSALL,[10] ROBERT M. LIGHT,[4] C. ROGER LYNDS,[2]
EARL J. O'NEIL, JR.,[2] DONALD P. SCHNEIDER,[11] EDWARD J. SHAYA,[6]
AND JAMES A. WESTPHAL[12]

Received 1990 October 17; accepted 1990 November 14

ABSTRACT

We have obtained *U*-band images of the M15 core with the Planetary Camera of the *Hubble Space Telescope*. We are able to resolve stars down to the main-sequence turnoff ($m_U \approx 19.4$) into the cluster center. We use crowded field photometry techniques to decompose M15 into bright resolved stars and a residual component consisting of stars at turnoff brightness or fainter. The residual component comprises 59% of the cluster light and follows a $\gamma = -0.71$ power-law distribution for $r > 1''$. The residual component flattens off interior to this radius and has a large core with $r_c = 2''.2 = 0.13$ pc. The core size may reflect postcollapse core expansion. The resolved stars have a slightly shallower distribution ($\gamma = -0.53$) but have an abrupt overdensity for $r < 1''.5$, which accounts for the unresolved surface brightness cusp at ground resolution. The bright stars do not become more highly concentrated at still smaller radii, however; neither the bright stars nor the residual component form a cusp at subarcsecond resolution. The total central density of light in all components is $8 \times 10^5\ L_\odot\ \mathrm{pc}^{-3}$ (*U*-band). The Peterson, Seitzer, and Cudworth central velocity dispersion implies a high core $M/L \approx 8$ (*U*-band). The existence of a core rather than a cusp at the 0.1 pc scale may imply that the centrally deduced dark matter is in a diffuse form rather than a massive black hole.

Subject headings: clusters: dynamics — clusters: globular

1. INTRODUCTION

M15 = NGC 7078 is the classic candidate for a cluster with a collapsed core. It has long been known that M15 is poorly fitted by King (1966) models (Newell & O'Neil 1978; Djorgovski & King 1984). No core or central leveling off of the light profile is evident from the ground; the distribution of light for $r < 10''$ instead follows a $\gamma = -0.62$ power law or "cusp" into the resolution limit (Lugger et al. 1987), consistent with multimass component models of cluster dynamical evolution (Murphy & Cohn 1988). While the general picture of M15 as a centrally collapsed cluster is accepted, its current state of evolution relative to the time of core bounce or maximum central density is still an open question. Recent work of Chernoff & Weinberg (1990) and Murphy, Cohn, & Hut (1990) shows that the light distribution may never form a cusp into arbitrarily small radii but instead will always maintain a core with finite size. The core radius, r_c (the point at which the brightness profile falls to half its central value), varies as the cluster evolves and appears to be a sensitive indicator of the mass spectrum and state of dynamical evolution. At the time of maximum collapse, the core can be as small as $r_c < 10^{-2}$ pc. For a distance to M15 of 12.8 kpc (Fahlman, Richer, & VandenBerg 1985), with implied scale $1''.0 = 6.2 \times 10^{-2}$ pc, this is $r_c < 0''.17$. After maximum collapse, the core may either expand freely or oscillate in size within an order of magnitude of this limit. M15 is thus a high-priority target for the *Hubble Space Telescope*.

We show here that despite the severe spherical aberration present in the *HST*, Wide Field/Planetary Camera (WFPC) images still present useful high-resolution information on this object. We are able to resolve stars in the M15 core down to the main-sequence turnoff and subtract them from the images. The remaining faint, unresolved stars form a diffuse background with a surprisingly large core ($r_c = 0.13$ pc). The existence of a large core interior to the power-law cusp may imply that M15 has evolved well past maximum core collapse and may rule out the presence of a massive central black hole as well.

2. OBSERVATIONS

HST observations of M15 were obtained on 1990 September 19 with the Planetary Camera (PC), the high-resolution mode of the WFPC. Detailed description of the camera is presented in Griffiths (1989). Briefly, the PC comprises four CCD cameras each imaging one-quarter of a $66'' \times 66''$ field of view. Each CCD has an 800×800 format with $0''.0437$ pixel^{-1}. Four 800 s integrations were obtained in filter F336W, which corre-

[1] Based on observations with the NASA/ESA *Hubble Space Telescope*, obtained at the Space Telescope Science Institute, which is operated by AURA, Inc., under NASA contract NAS 5-26555.

[2] Kitt Peak National Observatory, National Optical Astronomy Observatories. Operated by the Association of Universities for Research in Astronomy, Inc., under cooperative agreement with the National Science Foundation. Postal address: National Optical Astronomy Observatories, P.O. Box 26732, Tucson, AZ 85726.

[3] Lowell Observatory, 1400 Mars Hill Road, Flagstaff, AZ 86001.

[4] UCO/Lick Observatories, Board of Studies in Astronomy and Astrophysics, University of California, Santa Cruz, Santa Cruz, CA 95064.

[5] Astronomy Department, FM-20, University of Washington, Seattle, WA 98195.

[6] Department of Physics and Astronomy, University of Maryland, College Park, MD 20742.

[7] Space Telescope Science Institute, 3700 San Martin Drive, Baltimore, MD 21218.

[8] Physics Department, Box 708, Princeton University, Princeton, NJ 08544.

[9] Infrared Processing and Analysis Center, 100-22, California Institute of Technology, Pasadena, CA 91125.

[10] NASA/Goddard Space Flight Center, Laboratory for Astronomy and Solar Physics, Code 685, Greenbelt, MD 20771.

[11] Institute for Advanced Study, School of Natural Sciences, Olden Lane, Building E, Princeton, NJ 08590.

[12] Division of Geological and Planetary Sciences, 170-25, California Institute of Technology, Pasadena, CA 91125.

sponds roughly to the Johnson U band. The exposures were split into two pairs; the cluster center was positioned in CCD PC5 for one pair and PC6 for the other. Unfortunately, the pointing differed inadvertently by several arcseconds between the two exposures in each pair as well. The spacecraft was in fine lock for all observations. Observations were obtained in the U band in an attempt to suppress the strong luminosity fluctuations contributed by red giants to the composite cluster light. Unfortunately this is somewhat offset by the low sensitivity of the combined PC plus *HST* system in the U band. The average signal level in the central 1″ of M15 in the individual exposures is ~ 1000 photons pixel^{-1}. Sky background is negligible.

At the time of the observations, the WFPC was still in an uncalibrated state prior to the application of the "UV-flood." A combination of ground-test data and provisional on-orbit calibrations allowed most of the basic reduction steps outlined in Lauer (1989) to be completed. The main problems are flat-fielding and cosmic-ray removal. On-orbit flats have not yet been generated for the U filter, so preflood ground-test flats were used after correction for the test-lamp illumination pattern by comparisons between ground and orbit flats taken through filter F230W. Both PC5 and PC6 are fairly uniform over the regions of interest, and we find that the cluster light profile changes only slightly after flat-fielding. By an iterative process, cosmic-ray hits in one image in each pair were replaced by valid data from the other. The overlap between the exposures in each pair is about 400 × 400 pixels centered on the core of M15. After cosmic-ray removal, the images in each pair were registered and added using sinc interpolation to produce a final 400 × 400 pixel image for the two different PCs. Except as noted, subsequent analysis is carried out for the two PCs separately.

An image of the central 17.″2 × 17.″2 region of M15 is presented in the left-hand panel of Figure 1 (Plate L11) (all exposures were combined for this figure). A ×4 zoom on the residual light center of M15 as measured below is presented in the second panel in Figure 1. Individual stars resolved at the subarcsecond level are clearly visible in the M15 core. Figure 1 can be contrasted with the excellent ground based data of Racine & McClure (1989); even in 0.″35 seeing, the central stars remain unresolved. Outside of the central arcsecond in the present images, the brighter stars seem to be only weakly concentrated toward the center and indeed subjectively appear to be organized into a number of clumps. We emphasize that much of the diffuse light seen in Figure 1 is really the additive light of the strong wings of the PSF, which extend out to $\sim 3''$. In the present state of *HST*, only a small fraction of the light in the PSF (about 15%) goes into the sharp diffraction cores (Burrows et al. 1991).

The strong wings of the PSF plus the strong luminosity fluctuations introduced by the random distribution of bright stars makes analysis of the "parent" core light distribution challenging. Our approach is to first "clean" the image of bright stars, correct the resulting residual distribution of light for the PSF wings by deconvolution, and then measure its brightness profile with standard surface photometry techniques (such as those of Newell & O'Neil 1978). We then appeal to stability of the results over different decomposition methods and the strong constraint of total conservation of light to establish bounds on the uniqueness and accuracy of the results. We note here two other approaches that were attempted but found useless for understanding the M15 light distribution. Direct measurement of the raw total light profile suffers both from strong random fluctuations introduced by bright stars as well as strong blurring introduced by the PSF wings. Direct analysis of the image after PSF deconvolution corrects for the latter problem, but the variance introduced by the random placement of bright stars becomes even more severe. Instead, we identify the bright stars, set them aside, and get at the underlying smooth light distribution, which is really the most accurate indicator of the luminosity profile. The bright stars can then be considered or not in any subsequent analysis as warranted.

Decomposition of the image was done with the DAOPHOT stellar photometry package (Stetson 1987), as modified by Holtzman (1990) for WFPC applications. Stars were identified to a faint limit from the composite frame made by adding both PC images together, although the subsequent decompositions were done on the two PC images separately to allow intercomparison of the results. The PSF was taken from a bright star within the field. Plots of measured stellar brightness as a function of distance from the M15 core for both images show no strong radial bias in the completeness limit. A global luminosity cutoff was identified, and only stars above the threshold in both PCs were kept in the final star list. The morphology of the horizontal branch at $m_U = 16.37$ (Sandage 1970) is clearly visible in the luminosity function and is used to provide a photometric zero point. By coincidence, the adopted luminosity cutoff falls almost exactly at the main-sequence turnoff ($m_U \approx 19.4$).

The decomposition results are shown in Figures 2 (Plate L12) and 3. The left-hand panel in Figure 2 shows the DAOPHOT model of the light distribution of just the bright stars above the

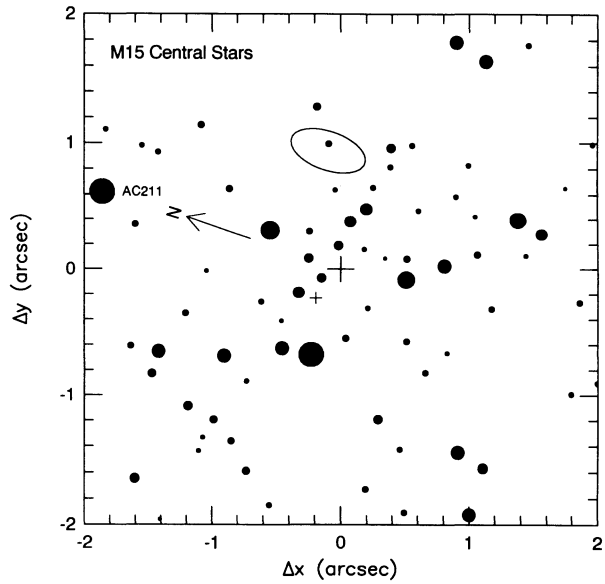

FIG. 3.—Schematic representation of the bright stars identified in the central 2″ × 2″ region surrounding the measured center of the residual light component. The area of the dots is proportional to the stars' U-band luminosities. The coordinate system refers to CCD rows and columns. Epoch 1950.0 coordinates of the center are $21^h27^m33^s.281 \pm 0^s.003$, $+11°56'49''.07 \pm 0''.04$. The rotation between CCD and celestial coordinates is 70°.8; east is to the lower part of the figure. The small cross marks the center measured by the reflected autocorrelation technique for total cluster light. AC 211 is the optical counterpart of the X-ray source 4U 2127+12 (Aurière, Le Fèvre, & Terzan 1984). The error ellipse at the location of PSR 2127+11A (Wolszczan et al. 1989) is also shown.

1991ApJ...369L..45L

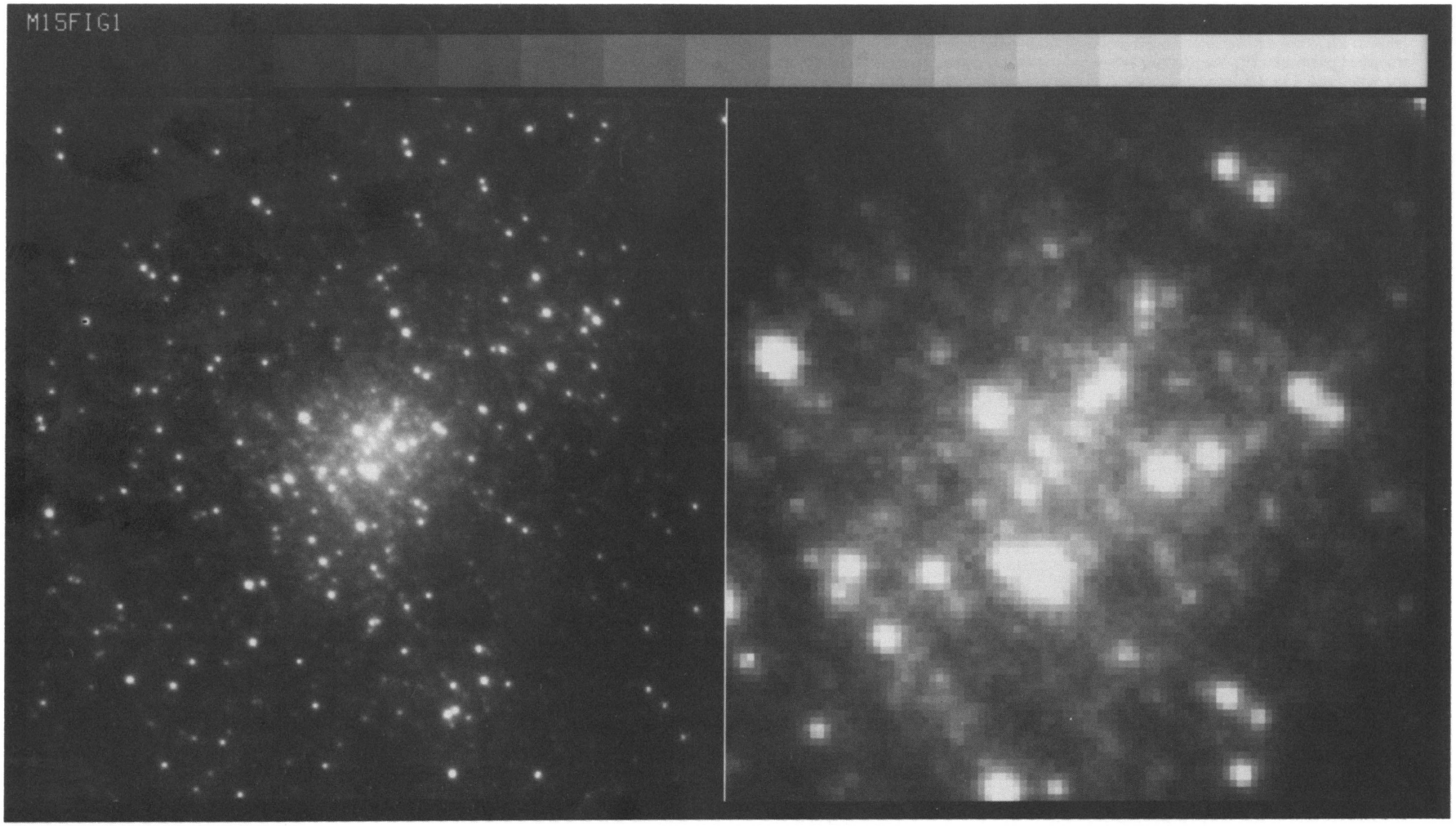

FIG. 1.—PC *U*-band image of M15. The left-hand panel shows the central 400 × 400 pixels or 17″.2 × 17″.2 region of the composite image made from co-adding all four 800 s exposures. See Fig. 3 for orientation. The gray scale is linear. The right panel is a ×4 zoom on the exact center as measured from the residual light. Stars have been resolved into the center.

LAUER et al. (see 369, L46)

1991ApJ...369L..45L

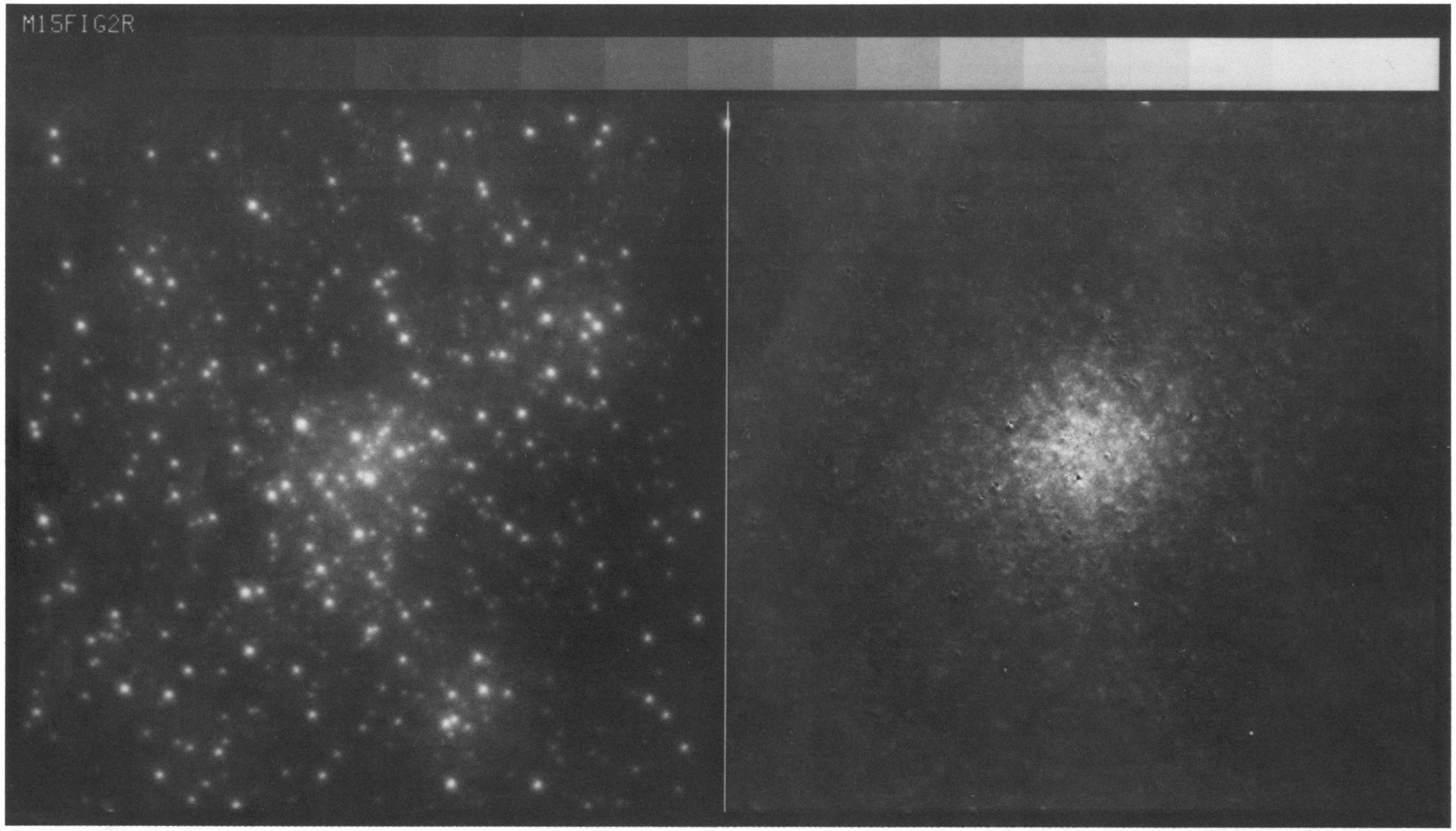

FIG. 2.—Bright star and residual light decomposition of M15. The left-hand panel shows the DAOPHOT model fit to just the bright stars with $m_v < 19.4$ in the central 400 × 400 pixels. All diffuse emission in the bright star image is thus due to the extended PSF wings. The gray scale is logarithmic to emphasize the shallow concentration of the bright stars. The right-hand pnael is a linear display of the residual light image generated by subtacting the bright star model in the left-hand panel from the original images. Note the smooth and symmetrical distribution of the residual light. See Fig. 3 for orientation.

luminosity cutoff; the diffuse light here, therefore, comes entirely from the PSF wings. Positions and magnitudes of those stars within the central 2″ around the core are shown schematically in Figure 3. The right-hand panel in Figure 2 shows the residual light of the unresolved, undetected stars (for display, both PC images have been added), which was generated by subtracting the model fit of the bright stars from the observations. The residual light is clearly "prickly," showing that it is composed in part of many barely resolved stars (as well as some sharp residuals from the cores of the brighter stars), but it is otherwise strikingly smoothly and symmetrically condensed about the center of M15. The distribution of the residual light is also extremely flat in the center. The brightness profile measured after the residual image was corrected by Lucy (1974) deconvolution, is shown in Figure 4. The increase in central surface brightness over deconvolution is small, with $\Delta\mu_0 \approx 0.^m3$ mag (Fig. 5). This is expected since the raw core is flat and about as extended as the PSF wings. The deconvolved residual profile can be described as a power law with slope $\gamma = -0.71$ for $r > 1''$, that quickly levels off to a constant central surface brightness core with $\mu_0 = 14.7$ mag arcsec^{-2} (U band) for $r < 0''.4$. The implied core size (half-power radius) of the residual light is $r_c = 2''.2$, or 0.13 pc.

The center of the residual light was measured by the reflected autocorrelation method (Djorgovski 1988) and is shown in Figure 3. For epoch 1950.0, the center is at $21^h27^m33^s.281 \pm 0^s.003$, $+11°56'49''.07 \pm 0''.04$, where the errors are based on comparison of the PC and PC6 images. The transformation from pixel coordinates to celestial coordinates was provided by the radio position (Kulkarni et al. 1990) of the X-ray source 4U 2127+12, which is identified with star AC 211 (Aurière, Le Fèvre, & Terzan 1984; see Fig. 3). The center measured here differs from the Shawl & White (1986) center by $\Delta\alpha = -1''.0$ and $\Delta\delta = +0''.3$. It is noteworthy that the position of the center does not coincide with any of the bright stars. The center deduced using all the cluster light (bright stars plus residual light) with $r < 2''.7$ is also shown in Figure 3. It is displaced from the residual light center but also does not fall at the location of any of the bright stars. There is no evidence that any single star in the core of M15 might be associated with the location of a possible cusp at subarcsecond scales. Last, in Figure 3 we give the error ellipse showing the location of the pulsar PSR 2127+11A (Wolszczan et al. 1989), which is only 0″.96 from the center position derived here. Figure 3 shows that one star falls within the error ellipse, although Figure 1 shows that this is really a blend of two stars, both with brightnesses close to the $m_U = 19.4$ cutoff.

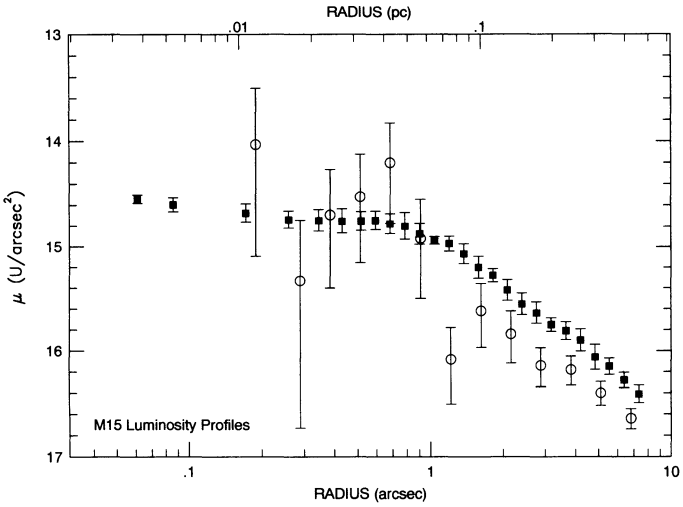

FIG. 4.—Surface brightness profiles measured for the residual light (*solid symbols*) and bright star (*open symbols*) components. Lucy (1974) deconvolution has been applied to the residual light image to correct for scattering by the PSF wings. The bright star profile is generated from the DAOPHOT photometry fit and thus can also be reviewed as a deconvolved brightness profile. The width of the bins for the bright star profile is twice their spacing to provide for smooth sampling of the profile. Error bars for the bright star profile are based on luminosity-weighted counting statistics. Error bars for the residual light profile are based on measuring the pixel intensity variance within the circular rings used to measure the brightness profile.

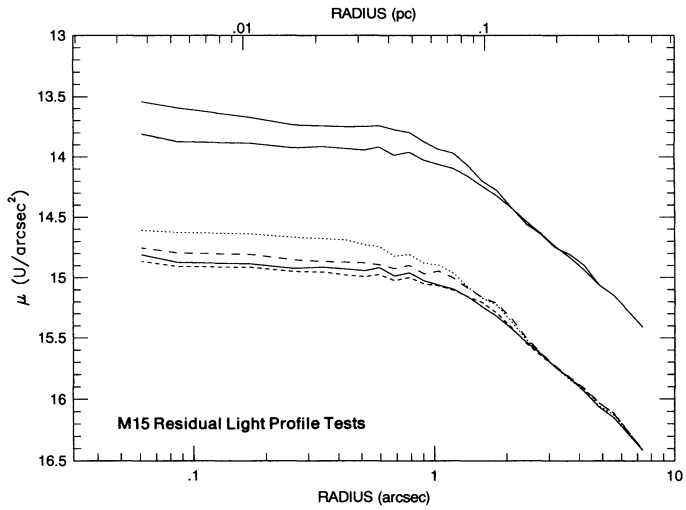

FIG. 5.—Residual light profile tests. The upper two traces show the residual light profile before and after Lucy (1974) deconvolution. The deconvolved profile is also shown in Fig. 4. Both profiles have been shifted up 1 mag for display. The lower set of traces show the raw (prior to deconvolution) residual light profiles that result from the different tests described in the text. The major effect of different decomposition attempts is to shift the residual light profile up or down in brightness. Here all profiles are normalized to the same brightness at large radii. The solid trace is the adopted raw profile repeated from the upper trace above. The dashed line slightly below the solid line results from a cutoff to the bright-star population 1 mag brighter than used. The dashed line above the solid line results from the "bad sky" experiment. The dotted line above this is the "incorrect PSF" experiment. This profile is steeper than the adopted profile for $1'' < r < 3''$ but otherwise has the same core structure.

We have used several different approaches to test the conclusion that the distribution of residual light in M15 flattens out at small radii. The most useful constraint is that total light must be conserved. One exercise is to consider what would be seen if there really were a cusp in the diffuse background that continued into small scales with $\gamma = -0.7$. The integrated brightness of the residual light for $r < 1''$ is $m_U = 13.5$. The predicted total luminosity for the $\gamma = -0.7$ cusp is $m_U \approx 13.2$ for $r < 1''$, which can be expressed as an additional central source of light with $m_U \approx 14.7$. The combined light of the two stars interior to $r < 0''.2$ (the two stars closest to the center cross in Fig. 3) is $m_U \approx 16.6$; only when we integrate out to the 10 stars with $r < 0''.5$ do we exceed the cusp requirement. In other words, to generate enough light for a cusp in the residual light would require gross misidentification of central bright stars at a level that is not possible. While the initial choice of brightness cutoff between the bright stars and the residual light was arbitrary, we also find that the exact completeness limit of the stellar sample is unimportant, within broad limits. Selecting the cutoff a full magnitude brighter, at $m_U = 18.4$, does not change the shape of the profile, only its total brightness by

$\Delta\mu_0 = 0.23$ (Fig. 5). The profiles from PC5 and PC6 separately also agree well.

Two other experiments were done to test sensitivity to PSF errors. The PSF star that we adopted (AC5 from the catalog of Aurière & Cordoni 1981) is the brightest star in the field and had wings that could be detected out to 2".2. AC5 is located ~14" from the cluster center, and there may be some question as to how well we have corrected for the presence of background cluster light at its location. To test this, we arbitrarily altered the PSF background level to the point that the image with bright stars subtracted developed obvious discontinuities at the boundaries of the PSF regions. The resultant profile of the residual light is substantially unchanged with only a slight shift in the zero point (Fig. 5). The last experiment was to use a PSF known to be incorrect, which we took from an image taken in a different filter (F368M). The star subtractions were clearly inferior to those using the adopted PSF and did yield a slightly more concentrated light profile interior to $r < 2''$; however, a large flat core was still observed. This and the other experiments shown in Figure 5 suggest that we cannot rule out a shallow power-law interior to $r < 1''$, but any slope appears certainly limited to $\gamma > -0.2$.

The one remaining question is why, with a large core in the residual light, M15 still shows a cusp in excellent ground-based seeing. The explanation appears to be in the distribution of bright, resolvable stars. The surface brightness profile generated from the bright stars is shown for comparison in Figure 4. For $r < 7''.34$, the distribution of bright stars has $\gamma = -0.52 \pm 0.08$ and thus may be slightly less concentrated than the residual light. Integrated over the inner $r < 7''.34$, the residual light has total $m_U = 10.3$, while the stars have $m_U = 10.6$, or 41% of the total light. However, the bright stars have a highly localized density enhancement for $r < 1''.5$, and for $0''.4 < r < 1''.0$ the integrated light of bright stars *exceeds* that of the residual background by $\Delta m_U \approx 0.4$. Thus, the diffuse core is swamped by the sudden rise in bright star surface density, creating the impression of an unresolved cusp from the ground. We emphasize, however, that the bright stars do not become even more concentrated at $r < 0''.5$ and do not form a cusp at *sub*arcsecond resolution. The significance of the central excess of bright stars is unclear. The central surface brightness of the resolved stars deviates from the residual core by less than 2 σ when the profiles are normalized at large radii and thus may be no more than a random fluctuation. Theoretical cluster models (Chernoff & Weinberg 1990; Murphy et al. 1990) furthermore do not predict a significant difference in the distribution of the bright stars and the residual light, as the mass difference between the stellar types is small ($<0.2\ M_\odot$). On the other hand, this rise occurs at a very special location and should not be lightly ignored. Whether or not the core stars are a special population of objects cannot be addressed by the current observations, which are only in one color. We do note, in passing, that several recent investigations argue that the population over roughly the area covered by our entire image differs from that in the outer regions of the cluster (see Stetson 1991 for a review).

3. DISCUSSION

The existence of a core in the diffuse light of M15 is in good agreement with recent revisions to the picture of core collapse in globular clusters. The light-emitting population is sufficiently disconnected dynamically from the dark population undergoing collapse that the visible light should show no cusp despite extreme condensation in the massive components. The tripartite light profile—flat core, intermediate power-law cusp, and outer tidal fall off—is equally well matched by either precollapse (Chernoff & Weinberg 1990) or postcollapse (Murphy, et al. 1990) models. However, given the short relaxation time in the core, $t_r \approx 14 \times 10^6$ yr (Peterson, Seitzer, & Cudworth 1989), we would presume that we are looking at a postcollapse cluster.

The question then is whether the M15 core will continue to expand forever or will undergo gravothermal oscillation. The dividing line between the two cases depends on the total cluster mass and stellar mass spectrum. A cluster luminosity $M_V = -9.27$ (Webbink 1985) and $M/L_V = 1.7$ (Peterson, et al. 1989) imply a cluster mass $M = 7.2 \times 10^5\ M_\odot$; with mass spectrum power $x = 2.5$ (Fahlman, et al. 1985), we would expect the core to oscillate, by naive comparison to the Murphy, et al. (1990) models. The cores of the oscillating models appear to stay limited to $r_c < 0.05$ pc, however, and the $\gamma = -0.71$ that we observe outside the core is smaller than the model $\gamma = -1.0$. Both of these discrepancies might be cured by suitable adjustment of the mass spectrum or cluster mass. We make no conclusion here but raise these suggestions to highlight the use of the observed diffuse core as an evolutionary diagnostic.

The present light profile may also constrain the mass of any central black hole or dark stellar remnants present in the M15 core. Peterson, et al. (1989) observe a central $\sigma \approx 25$ km s^{-1} and argue for a central $10^3\ M_\odot$ black hole based on their strongly nonisothermal dispersion profile. With $\mu_0 = 14.7$ mag arcsec^2 and $r_c = 0.13$ pc, we find $\rho_0 = 3.8 \times 10^5\ L_\odot$ pc^{-3}, assuming $M_U = 5.61$ for the Sun (Allen 1973). If we double the central light density to account for the bright stars, then we get $M/L_U \approx 8$ in the core. This is clearly higher than the global cluster M/L for M15 noted above and indeed argues for the presence of some dark matter in the M15 core. The question is whether the existence of a core rather than cusp for $r < 0.1$ pc is more consistent with dark matter in a diffuse form rather than as a centrally condensed object. If the black hole is massive enough, then the high orbital velocities in its neighborhood will shut off significant energy exchange between members of the surrounding stellar population. In this case, the core will not be able to expand after core collapse, nor will any mechanism be able to destroy the dense mass cusp presumably associated with formation of the black hole in the first place. We thus favor the dark matter in a diffuse rather than singular form.

This research was conducted by the WFPC Investigation Definition Team operating under partial support from NASA contract NAS5-25421.

REFERENCES

Allen, C. W. 1973, Astrophysical Quantities (London: Athlone)
Aurière, M., & Cordoni, J.-P. 1981, A&AS, 46, 347
Aurière, M., Le Fèvre, O., & Terzan, A. 1984, A&A, 128, 415
Burrows, C., Holtzman, J. A., Faber, S. M., Bely, P., Husan, H., Lynds, C. R., & Schroeder, D. 1991, ApJ, 369, L21
Chernoff, D. F., & Weinberg, M. D. 1990, ApJ, 351, 121
Djorgovski, S. 1988, in IAU Symposium 126, Globular Cluster Systems in Galaxies, ed. J. E. Grindlay & A, G. D. Philip (Dordrecht: Kluwer), 333
Djorgovski, S., & King, I. R. 1984, ApJ, 277, L49
Fahlman, G. G., Richer, H. B., & VandenBerg, D. A. 1985, ApJS, 58, 225
Griffiths, R. 1989, Wide Field and Planetary Camera Instrument Handbook, STScI publication

Holtzman, J. A. 1990, PASP, 102, 806
King, I. R. 1966, AJ, 71, 64
Kulkarni, S. R., Goss, W. M., Wolszczan, A., & Middleditch, J. M. 1990, ApJ, 363, L5
Lauer, T. R. 1989, PASP, 101, 445
Lucy, L. B. 1974, AJ, 79, 745
Lugger, P. M., Cohn, H., Grindlay, J. E., Bailyn, C. D., & Hertz, P. 1987, ApJ, 320, 482
Murphy, B. W., & Cohn, H. C. 1988, MNRAS, 323, 835
Murphy, B. W., Cohn, H. C., & Hut, P. 1990, MNRAS, 245, 335
Newell, B., & O'Neil, E. J. 1978, ApJS, 37, 27
Peterson, R. C., Seitzer, P., & Cudworth, K. M. 1989, ApJ, 347, 251
Racine, R., & McClure, R. D. 1989, PASP, 101, 731
Sandage, A. 1970, ApJ, 162, 841
Shawl, S. J., & White, R. E. 1986, AJ, 91, 312
Stetson, P. B. 1987, PASP, 99, 191
——. 1991, in Precision Photometry, ed. A. G. D. Philip (Schenectady: L. Davis), in press
Webbink, R. F. 1985, in IAU Symposium 113, Dynamics of Star Clusters, ed. J. Goodman & P. Hut (Dordrecht: Reidel), 361
Wolszczan, A., Kulkarni, S. R., Middleditch, J. M., Backer, D. C., Fruchter, A. S., & Dewey, R. J. 1989, Nature, 337, 531